JOURNAL OF OPTIMIZATION THEORY AND APPLICATIONS: Vol. 17, Nos. 5/6, 1975

Optimum Coasting Flight in a Horizontal Plane[1]

N. X. VINH[2] AND C. J. SHIEH[3]

Communicated by A. Miele

Dedicated to Professor A. Busemann

Abstract. Busemann's concept of optimum altitude for rectilinear coasting flight has been extended to flight in a horizontal plane. The reachable domain of a vehicle in coasting flight in a horizontal plane, starting from an initial velocity, is obtained. It is shown that the area covered first increases with the altitude and then decreases to zero when the ceiling is reached. In particular, there exists an altitude for maximum longitudinal range and another altitude for maximum lateral range. Optimum variations in the lift coefficient and the bank angle to reach the boundary of the footprint are discussed.

Key Words. Flight mechanics, coasting flight, horizontal flight, optimum trajectories, maximum longitudinal range, maximum lateral range.

1. Introduction

In Ref. 1, Busemann, Vinh, and Culp have solved the following problem. Consider a hypervelocity vehicle, coasting along a horizontal line with an initial speed V_0. As the speed decreases, in order to maintain the horizontal flight by using the lift to exactly balance the constant weight, the angle of attack has to be increased continuously through action on the elevator control until a maximum angle of attack is reached.

[1] This work has been supported in part by the Air Force Office of Scientific Research under Grant No. AF-AFOSR-71-2129.

[2] Professor, Department of Aerospace Engineering, The University of Michigan, Ann Arbor, Michigan.

[3] Graduate Student, Department of Aerospace Engineering, The University of Michigan, Ann Arbor, Michigan.

Let X_f be the final range obtained. It is shown that X_f is a function of the altitude; and, under a certain condition given explicitly, there exists an optimum altitude giving the maximum X_f. This optimum altitude is obtained by solving a transcendental equation. The problem has been solved for the flat Earth model, and also for the general case of a spherical Earth when the flight altitude is small as compared to the radius of the Earth.

In this paper, we extend the problem to the case of flight in a horizontal plane. At a given altitude, a vehicle possesses an initial horizontal velocity $\vec{V}_0$ resulting in an initial kinetic energy. With this initial energy, the vehicle can coast-flight in the horizontal plane passing through its initial velocity vector by varying the angle of attack and the bank angle. The flight is terminated when the velocity reaches a minimum value, which is just enough to sustain horizontal flight while using the maximum angle of attack. For each given altitude, it is proposed to find the domain which can be reached by the vehicle. This domain will be referred to as the footprint in horizontal coasting flight. Next, we shall consider the variation of the footprint with respect to the altitude; then, in some sense, we shall find the optimum altitude for coasting flight.

The problem, as formulated, is solved by using optimal control theory to find the lift and the bank angle programs with which the vehicle can reach the boundary of the footprint. Because of the complexity of the problem (namely, finding unknown functions by variational technique, rather than unknown discrete values as in the case considered in Ref. 1), we shall restrict ourselves to the case of flight using a flat Earth model. On the other hand, it will be shown that, through the use of a set of dimensionless variables, it is possible to give the complete solution to the problem, applicable to all types of vehicles, by specifying only two aerodynamic parameters, namely the maximum lift coefficient, and the maximum lift-to-drag ratio.

2. Equations of Motion

The equations of motion for a coordinated turn in a horizontal plane, with the engine shut off at all time, are (Ref. 2)

$$\begin{aligned} dX/dt &= V\cos\beta, \\ dY/dt &= V\sin\beta, \\ dV/dt &= -D/m, \\ V(d\beta/dt) &= L\sin\sigma/m; \end{aligned} \tag{1}$$

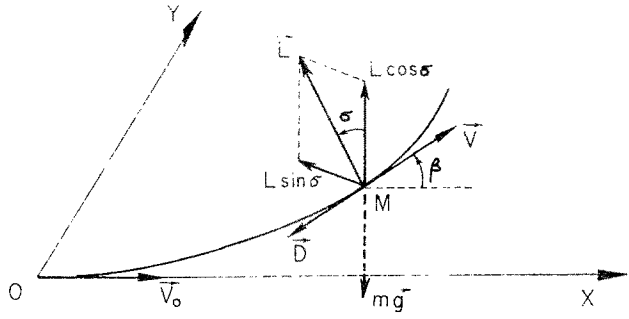

Fig. 1. Geometry of the trajectory.

here, besides the usual notation, we have used β for the heading and σ for the bank angle (Fig. 1). The X-axis is taken along the initial velocity $\vec{V}_0$.

For a coordinated turn at constant altitude, we have the constraining relation

$$L \cos \sigma = mg. \tag{2}$$

We shall use a parabolic drag polar of the form

$$C_D = C_{D0} + kC_L^2, \tag{3}$$

where the zero-lift drag coefficient C_{D0} and the induced drag factor k are assumed independent of the Mach number and the Reynolds number. We shall use the usual assumption for the lift and drag forces, that is,

$$L = \tfrac{1}{2}\rho S C_L V^2, \qquad D = \tfrac{1}{2}\rho S C_D V^2. \tag{4}$$

It is convenient to introduce the following dimensionless quantities:

$$\begin{aligned} u &= (V/V_0)^2, \qquad x = (\eta\rho S C_{D0}/m)X, \qquad y = (\eta\rho S C_{D0}/m)Y, \\ w &= mg/\eta\rho S C_{D0} V_0^2, \qquad \eta = 1/2\sqrt{(kC_{D0})} = \max(L/D). \end{aligned} \tag{5}$$

We notice that w is the apparent dimensionless weight. Although it is a constant for coasting flight in a horizontal plane, it increases with the altitude through the variation of the atmospheric mass density ρ. If the angle of attack, or equivalently the lift coefficient C_L, is not constrained, a natural choice for the aerodynamic control would be the bank angle σ. Then, the lift and the drag coefficients will be obtained from Eqs. (2) and (3). In practice, the lift coefficient is bounded and the corresponding bound on the bank angle is a function of the speed V through the constraining relation (2). Hence, the lift coefficient will be a better choice as control parameter in this case.

We define a lift control parameter λ such that λ^2 is the ratio of the induced drag to the zero-lift drag. This ratio is usually referred to as the drag ratio (Ref. 2). We have

$$\lambda = (k/C_{D0})^{1/2} C_L. \tag{6}$$

We notice that λ can be seen as the lift coefficient scaled such that $\lambda = 1$ corresponds to maximum lift-to-drag ratio. In terms of the new control variable λ, we have the drag coefficient

$$C_D = C_{D0}(1 + \lambda^2), \tag{7}$$

and the bank angle, through relations (2) and (5),

$$\cos \sigma = w/\lambda u, \qquad \sin \sigma = (\lambda^2 u^2 - w^2)^{1/2}/\lambda u. \tag{8}$$

Now, using u as the independent variable, the state equations (1) become, in dimensionless form,

$$\begin{aligned} dx/du &= -\eta \cos \beta/u(1 + \lambda^2), \\ dy/du &= -\eta \sin \beta/u(1 + \lambda^2), \\ d\beta/du &= -\eta(\lambda^2 u^2 - w^2)^{1/2}/u^2(1 + \lambda^2). \end{aligned} \tag{9}$$

In the equations of motion, w is a constant and can be used as a parameter. On the other hand, λ is the independent control variable. It is subject to the constraint

$$\lambda \leqslant \lambda_M . \tag{10}$$

3. Variational Equations

Let w denote a parameter specifying the flight altitude through ρ. For each altitude level, the flight starts at

$$u_0 = 1, \qquad x = 0, \qquad y = 0, \qquad \beta = 0. \tag{11}$$

The boundary of the footprint is reached by controlling optimally the lift λ until the limiting condition for horizontal flight is reached. By the constraining relations (8) and (10), we have the final condition

$$u_f = w/\lambda_M , \qquad x = x_f , \qquad y = y_f , \qquad \beta = \beta_f . \tag{12}$$

As a consequence, the bank angle always tends to zero on the boundary of the footprint with $\lambda = \lambda_M$. In this problem, the final heading β_f is

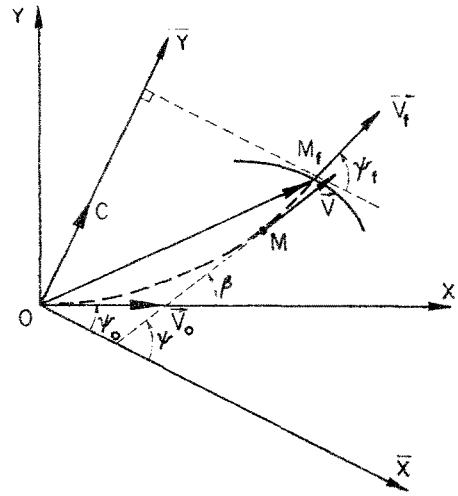

Fig. 2. Coordinate transformation.

free, while the final position (x_f, y_f) is optimized in some manner. One way to trace the footprint is to specify x_f while maximizing y_f. For reasons which will be clear below, we choose instead to maximize a performance index of the form

$$J = ax_f + by_f \tag{13}$$

for a prescribed pair of values a and b.

Let $\vec{OC}$ be the vector with components a and b (Fig. 2). Let $\vec{OM}_f$ be the final position vector of the vehicle. To maximize the dot product $J = \vec{OC} \cdot \vec{OM}_f$ for each prescribed vector $\vec{OC}$, the point M_f must be selected on the boundary of the footprint such that the tangent at M_f to the footprint is orthogonal to the vector $\vec{OC}$. Hence, by a rotation of axes such that the new axis $O\bar{y}$ is in the direction of $\vec{OC}$, the problem becomes that of maximizing $\bar{y}_f$ while $\bar{x}_f$ is free.

In the new coordinate system $O\bar{x}\bar{y}$, we have the equations

$$\begin{aligned} d\bar{x}/du &= -\eta \cos\psi/u(1+\lambda^2), \\ d\bar{y}/du &= -\eta \sin\psi/u(1+\lambda^2), \\ d\psi/du &= -\eta(\lambda^2u^2 - w^2)^{1/2}/u^2(1+\lambda^2), \end{aligned} \tag{14}$$

with the new heading angle ψ measured from the $\bar{x}$-axis. To write the variational equations for the maximizing problem, we introduce the vector (p_1, p_2, p_3) to form the Hamiltonian

$$H = -[\eta/u(1+\lambda^2)][p_1 \cos\psi + p_2 \sin\psi + (p_3/u)(\lambda^2u^2 - w^2)^{1/2}]. \tag{15}$$

The adjoint components p_i are defined by the equations

$$\begin{aligned} dp_1/du &= 0, \\ dp_2/du &= 0, \\ dp_3/du &= -[\eta/u(1+\lambda^2)](p_1 \sin\psi - p_2 \cos\psi). \end{aligned} \tag{16}$$

The performance index has been seen to be

$$J = \bar{y}_f, \tag{17}$$

with the end conditions

$$\begin{aligned} u_0 = 1, \quad \psi = \psi_0, \quad \bar{x} = 0, \quad \bar{y} = 0, \\ u_f = w/\lambda_M, \quad \psi_f = \text{free}, \quad \bar{x}_f = \text{free}, \quad \bar{y}_f = \max. \end{aligned} \tag{18}$$

From these conditions, we have

$$p_1(u_f) = 0, \quad p_2(u_f) = 1, \quad p_3(u_f) = 0. \tag{19}$$

Since the independent variable u is decreasing, the solution is obtained by integrating the systems of state equations (14) and adjoint equations (16), using the end conditions (18) and (19) with a lift control λ_{opt} subject to the constraint (10) and selected such that, at each instant, the Hamiltonian defined by (15) is an absolute maximum.

4. Optimal Lift Control

The adjoint system (16) is completely integrable. First, we have

$$p_1 = a_1, \quad p_2 = a_2, \tag{20}$$

where the a_i are constant. Using Eqs. (14) and (20), we can write the equation for p_3 as follows:

$$dp_3/du = d(a_1\bar{y} - a_2\bar{x})/du.$$

Hence, by integrating, we have

$$p_3 = a_1\bar{y} - a_2\bar{x} + a_3. \tag{21}$$

From the transversality condition (19), it is seen that

$$a_1 = 0, \quad a_2 = 1, \quad a_3 = \bar{x}_f. \tag{22}$$

Hence, we have

$$p_3 = \bar{x}_f - \bar{x}. \tag{23}$$

The Hamiltonian becomes

$$H = -[\eta/u^2(1+\lambda^2)][u\sin\psi + (\bar{x}_f - \bar{x})(\lambda^2u^2 - w^2)^{1/2}]. \tag{24}$$

The Hamiltonian, considered as a function of λ^2, is maximized when $\lambda = \lambda_M$ or at an interior point given by

$$(\bar{x}_f - \bar{x})\Lambda^2 + 2u\sin\psi\Lambda - (\bar{x}_f - \bar{x})(u^2 + w^2) = 0, \tag{25}$$

where we have defined

$$\Lambda = (\lambda^2u^2 - w^2)^{1/2}. \tag{26}$$

The positive root of the quadratic equation (25) is

$$\Lambda = [-u\sin\psi + [u^2\sin^2\psi + (\bar{x}_f - \bar{x})^2(u^2 + w^2)]^{1/2}]/(\bar{x}_f - \bar{x}). \tag{27}$$

Hence, the variable lift control λ (or, equivalently, Λ) is expressed explicitly in terms of the state variables and a constant $\bar{x}_f$. The variational problem is solved, and a numerical integration of the state equations will yield the optimal trajectory sought.

5. Reachable Domain

Since the optimal lift control has been obtained in terms of the state variables, the state equations (14) can be integrated numerically; and, at each altitude level w, the final position $(\bar{x}_f, \bar{y}_f)$ will describe the boundary of the footprint in the horizontal plane. The initial heading ψ_0 with respect to the $\bar{x}$-axis can be used as a scanning parameter (Fig. 2). Each angle ψ_0 provides an optimal trajectory leading to a point M_f on the boundary of the footprint. We notice that $\psi_0 = 0$ gives the final point with maximum lateral range, while $\psi_0 = 90°$ will give the final point on the x-axis with maximum longitudinal range.

In a forward integration, the parameter $\bar{x}_f$ in the optimal law (27) is unknown. Hence, a first guess is required, followed by an iteration process to match the end condition. To avoid this difficulty, we integrate the equations backward, as used by Fave in Ref. 3. Then, the final heading ψ_f is used as a scanning parameter with the following initial condition for the integration:

$$\text{at} \quad u = w/\lambda_M, \qquad \bar{x} = 0, \qquad \bar{y} = 0, \qquad \psi = \psi_f. \tag{28}$$

The initial lift is always $\lambda = \lambda_M$, and subsequent lift control is obtained from Eq. (26) as

$$\lambda^2 = (w^2 + \Lambda^2)/u^2, \tag{29}$$

with Eq. (27) for Λ now becoming

$$\Lambda = \{-u \sin \psi + [u^2 \sin^2 \psi + \bar{x}^2(u^2 + w^2)]^{1/2}\}/\bar{x}. \tag{30}$$

The integration stops at $u = 1$, providing a set of values ψ_0, $\bar{x}_f$, $\bar{y}_f$. The coordinates of the position M_f on the footprint, in the original Oxy coordinate axes, will be given by

$$x_f = -\bar{x}_f \cos \psi_0 - \bar{y}_f \sin \psi_0, \qquad y_f = \bar{x}_f \sin \psi_0 - \bar{y}_f \cos \psi_0. \tag{31}$$

The numerical integration requires specifying only two aerodynamic parameters, namely the maximum drag ratio λ_M and the maximum lift-to-drag ratio η. The values used were $\lambda_M = 1.4$ and $\eta = 2$, which are typical for a high-speed vehicle with moderate lift capability. Figure 3 plots the footprint for different flight levels; w varies from a small positive value to the limiting value $w = \lambda_M$ defining the ceiling. At this altitude, as discussed in Ref. 1, the lift capability is not sufficient to maintain level flight, and the footprint is reduced to a point. The footprint varies with the altitude through the apparent weight w. In the plots, the true coordinates have been recovered through the transformation (5), written as

$$X/(V_0^2/g) = wx, \qquad Y/(V_0^2/g) = wy. \tag{32}$$

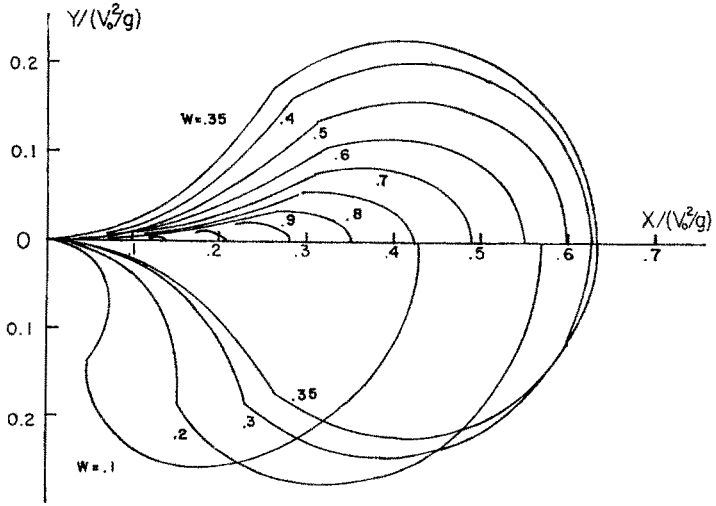

Fig. 3. Footprint as a function of the altitude.

The lower half of the figure plots the half footprints at low altitude ($w \leqslant 0.35$), and the upper half plots the half footprints at high altitude ($w \geqslant 0.35$), until the ceiling ($w = 1.4$). The generality of the analysis is clear, since the results are independent of the initial speed and the other characteristics of the vehicle. By varying V_0, we vary proportionally the size of the footprint. The wing loading mg/S and the zero-lift drag coefficient C_{D0} of any specified vehicle have been included in the altitude parameter w.

Typical footprint and optimal trajectories leading to its boundary are presented in Fig. 4, using the value $w = 0.35$. This altitude level is near the altitude giving the maximum longitudinal range. The exact value of this critical altitude level can be computed for any given λ_M from the transcendental equation (Ref. 1)

$$2/(1 + w^2) = \log[\lambda_M^2(1 + 1/w^2)/(1 + \lambda_M^2)]. \tag{33}$$

In the integration process, whenever λ as obtained from Eq. (27) is larger than λ_M, the control $\lambda = \lambda_M$ is used and the corresponding bank angle reaches its instantaneous maximum permissible value. To reach any point along the boundary of the footprint, from the point A to the point B, the trajectory is flown with variable lift coefficient λ which increases from an initial value to the final value λ_M. Points on the boundary of the footprint between the points B and C are reached by using a variable lift program which decreases first and then increases until the final value λ_M. Points on the boundary between the points C and D are reached by flying initially with $\lambda = \lambda_M$, along the path $0D$. At a point called the switching point, the trajectory leaves the arc $0D$ tangentially, and the final arc is flown with variable lift coefficient. Finally, the limiting arc $0D$ is entirely flown with $\lambda = \lambda_M$. The point $*$ on the footprint is the point with maximum lateral range. The variations of the

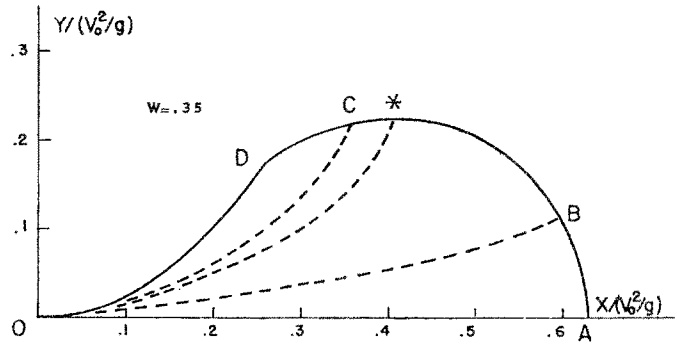

Fig. 4. Characteristic points on the footprint.

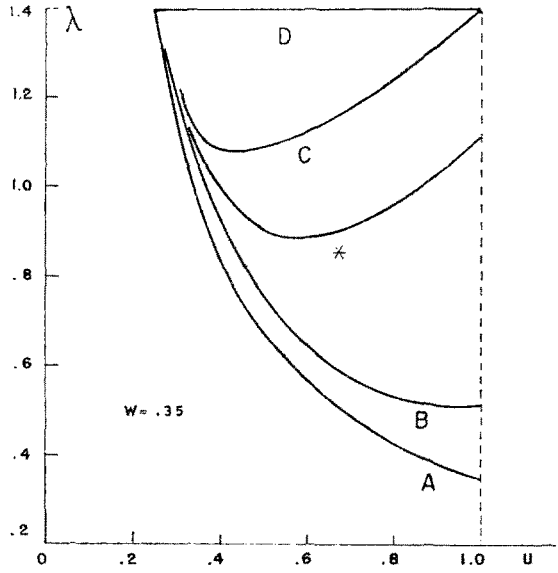

Fig. 5. Variation of the optimal lift coefficient.

lift coefficient λ are shown in Fig. 5, while Fig. 6 presents the variations of the bank angle σ. In Fig. 7, which plots the variations of the maximum longitudinal range and the maximum lateral range as w varies, it is seen

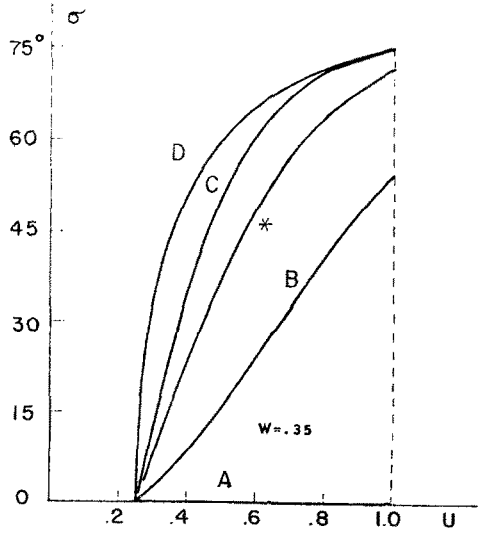

Fig. 6. Variation of the optimal bank angle.

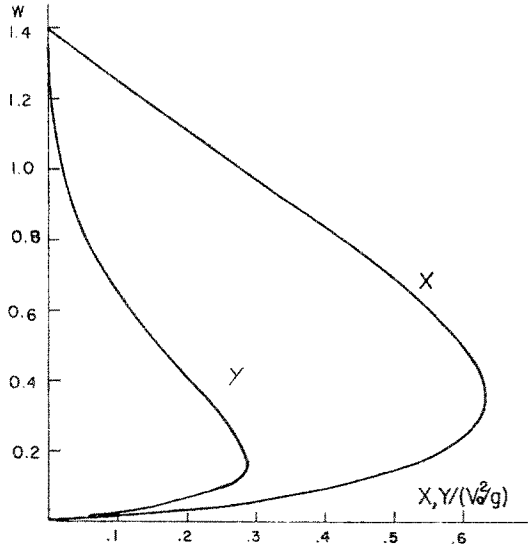

Fig. 7. Maximum longitudinal and lateral ranges as functions of the altitude.

that there exists a flight level w giving the longest maximum longitudinal range and another flight level giving the largest maximum lateral range. While, as shown in Ref. 1, the altitude level w for maximum longitudinal range is a function of only the characteristic value λ_M, and can be obtained from the explicit transcendental equation (33), the critical flight level w for maximum lateral range is a function of both the maximum drag ratio $\lambda_M{}^2$ and the maximum lift-to-drag ratio η. The exact value of this critical altitude can be obtained through a numerical integration scheme, as will be presented in the next section.

One distinctive feature of this analysis is that the altitude is represented by the apparent dimensionless weight w. This device, as suggested by Busemann (Ref. 1), who apparently is inspired by similar dimensionless variables proposed by Miele (Ref. 2), not only permits a general discussion independent of the wing loading mg/S and the zero-lift drag coefficient C_{D0} of any specified vehicle, but also has provisions for a general type of atmosphere. The only assumption is that ρ is a decreasing function of the altitude. This assumption results in a ceiling for the reachable domain. For any flight level w, for any specified type of vehicle using an initial speed V_0, the actual altitude is obtained through the transformation

$$\rho = (mg/S)/\eta w C_{D0} V_0{}^2. \tag{34}$$

In Fig. 7, it is seen that both the maximum longitudinal range and the maximum lateral range tend to zero when w tends to zero. Let ρ_0 be the atmospheric mass density at sea level. Then, for any prescribed vehicle, using any initial speed V_0, the minimum value of w can be obtained from Eq. (34), and Fig. 7 can be used to detect whether or not critical altitudes exist for the longest maximum longitudinal range or the largest maximum lateral range. Also, it is seen that, if the minimum of w is small enough, the maximum area covered first increases with the altitude and then decreases to zero when the ceiling is reached.

6. Some Related Problems

6.1. Maximizing the Final Speed. Consider the motion at a specified flight level w (Fig. 4). While the trajectory leading to any prescribed point M_f on the boundary of the footprint is unique, points inside the footprint can be reached by an infinite number of flight paths. Consequently, we can formulate the following problem: find the optimal trajectory leading to a prescribed position $M_f(x_f, y_f)$ with a maximum final speed.

The problem is solved by using the original set of state equations (9). The adjoint equations are the same as Eqs. (16), with ψ replaced by β. The final position is prescribed, while the final heading is free. Hence,

$$p_1 = a_1, \qquad p_2 = a_2, \qquad p_3 = a_2(x_f - x) - a_1(y_f - y). \tag{35}$$

The optimal lift control is either λ_M or as given by the equation for Λ,

$$\Lambda = (\lambda^2 u^2 - w^2)^{1/2},$$

which now becomes

$$[n(x_f - x) - (y_f - y)]\Lambda^2 + 2u(\cos\beta + n\sin\beta)\Lambda - [n(x_f - x) - (y_f - y)](u^2 + w^2) = 0, \tag{36}$$

where

$$n = a_2/a_1, \qquad a_1 \neq 0. \tag{37}$$

First, we consider the case where the trajectory is entirely flown with variable lift coefficient. If the state equations are integrable analytically, then using the end conditions (11) and (12) with u_f and β_f arbitrary and x_f and y_f prescribed, we have three equations which can be solved for the unknowns n, β_f, and the final maximized speed u_f.

Since numerical integration is required in this problem, a guessed value for n has to be used in Eq. (36). Instead of using n as a parameter, we can use the initial lift coefficient λ_i as parameter. Then, from Eq. (36), we have the corresponding value for n:

$$n = (1/x_f)[y_f + 2\sqrt{(\lambda_i^2 - w^2)/(1 + 2w^2 - \lambda_i^2)}]. \tag{38}$$

The following scheme has been tested with excellent results. First, we have a guessed value for λ_i, generally between 1 and λ_M. Then, n is obtained from Eq. (38); and, using the control law (36), we integrate the state equations from the initial condition, using $x = x_f$ as stopping condition. The resulting value for y is compared with the prescribed value y_f, and necessary correction in n is made until the prescribed final condition is met.

The procedure is valid for the case where the optimal trajectory is composed of an initial arc flown with λ_M, followed by an arc with variable lift. In this case, the iteration process described above leads the initial λ_i to λ_M. Then, we use a guessed value for n, sensibly larger than the value computed by Eq. (38) with $\lambda_i = \lambda_M$. The state equations are integrated with $\lambda = \lambda_M$, from $u = 1$ until $u = u_s$, such that the following condition is satisfied:

$$[n(x_f - x_s) - (y_f - y_s)]\Lambda_M^2 + 2u_s(\cos\beta_s + n\sin\beta_s)\Lambda_M - [n(x_f - x_s) - (y_f - y_s)](u_s^2 + w^2) = 0, \tag{39-1}$$

with

$$\Lambda_M = (\lambda_M^2 u_s^2 - w^2)^{1/2}. \tag{39-2}$$

At this point, called the switching point, we change to a variable lift program using the optimal control law (36) and continue the integration until $x = x_f$. The resulting value for y is compared with the prescribed y_f, and necessary correction in n is made until the prescribed final condition is satisfied.

If the point M_f is located exactly at either one of the characteristic points A, B, C, or D, the final speed is known, $u_f = w/\lambda_M$. The respective optimal program for λ is as follows.

Point A. The bank angle is zero, and $\lambda = w/u$ (Ref. 1).

Point B. This point is characterized by the additional condition $d\lambda/du = 0$, at $u = 1$ (Fig. 5). Hence, first by evaluating Eq. (36) at the initial point, we have

$$(nx_f - y_f)\Lambda_i^2 + 2\Lambda_i - (nx_f - y_f)(1 + w^2) = 0, \tag{40}$$

where

$$\Lambda_i = (\lambda_i^2 - w^2)^{1/2}$$

and λ_i is the initial lift coefficient. Next, by taking the derivative of Eq. (36) and then evaluating it at the initial point, we have

$$2(nx_f - y_f)\Lambda_i^3 + 4\Lambda_i^2 + [2(nx_f - y_f)(w^2 - 1) - n\eta]\Lambda_i + 2w^2 = 0. \quad (41)$$

The last two equations can be solved for the unknowns n and Λ_i. We have, by combining the equations,

$$n = 2w^2(1 - 2y_f\Lambda_i)/(\eta - 4w^2x_f)\Lambda_i. \quad (42)$$

By substituting into Eq. (40), we have a cubic equation for Λ_i:

$$\eta y_f\Lambda_i^3 - 2(\eta - 3w^2x_f)\Lambda_i^2 - \eta y_f(1 + w^2)\Lambda_i + 2w^2x_f(1 + w^2) = 0. \quad (43)$$

Point C. This point is characterized by the fact that, at $u = 1$, $x = y = \beta = 0$, the variable lift coefficient computed from Eq. (36) is $\lambda = \lambda_M$. Hence, we have for the value of n:

$$n = (1/x_f)[y_f + 2\Lambda_M/(1 + w^2 - \Lambda_M^2)], \quad (44\text{-}1)$$

where

$$\Lambda_M = (\lambda_M^2 - w^2)^{1/2}. \quad (44\text{-}2)$$

Point D. This point is obtained by flying constantly at maximum lift coefficient $\lambda = \lambda_M$. The final heading angle is given by

$$\beta_f = [\eta/(1 + \lambda_M^2)][\lambda_M \log\{[\lambda_M + (\lambda_M^2 - w^2)^{1/2}]/w\} - (\lambda_M^2 - w^2)^{1/2}]. \quad (45)$$

6.2. Maximizing the Lateral Range. *Point* $\divideontimes$. In this problem, the final x_f is free, while the final y_f is maximized. Hence, the condition (35) becomes

$$p_1 = 0, \qquad p_2 = 1, \qquad p_3 = x_f - x. \quad (46)$$

If variable lift control is used, it is obtained from

$$(x_f - x)\Lambda^2 + 2u \sin\beta\Lambda - (x_f - x)(u^2 + w^2) = 0. \quad (47)$$

At low altitude, the point $\divideontimes$ is between the points A and C, and pure variable lift is used. Next, as the altitude level increases, the point $\divideontimes$ is reached by flying first at $\lambda = \lambda_M$ and then switching to variable λ.

To evaluate the point with maximum lateral range on the footprint, let us first consider the case where pure variable lift is used. The equation

(47) is used for the lift control with a guessed value for x_f, and the states equations are integrated until $u = w/\lambda_M$. The resulting final value for x is compared with the guessed value for x_f, and necessary correction is made until the difference becomes zero. We notice from Eq. (47) that the initial lift coefficient is always

$$\lambda_i^2 = 1 + 2w^2. \tag{48}$$

Hence, it is a function of the flight level only.

If an initial arc using the maximum lift coefficient is involved, it is reflected by the fact that the initial lift computed by Eq. (48) is larger than λ_M. Hence, we have the criterion

$$w \geqslant [(\lambda_M^2 - 1)/2]^{1/2}. \tag{49}$$

To compute the trajectory leading to the point with maximum lateral range above this flight level, we also use a guessed value for x_f, but the state equations (9) are first integrated with $\lambda = \lambda_M$ until the following switching condition is satisfied:

$$(x_f - x_s)(\lambda_M^2 u_s^2 - w^2) + 2u_s \sin\beta_s(\lambda_M^2 u_s^2 - w^2)^{1/2} - (x_f - x_s)(u_s^2 + w^2) = 0. \tag{50}$$

At this point, variable lift control as given by Eq. (47) is used, and the iteration with respect to x_f is done as before. The results are plotted in Fig. 7 for maximum lateral range.

6.3. Footprint for Prescribed Final Speed. We have defined the footprint in a horizontal plane as the reachable domain using a prescribed initial velocity $\vec{V}_0$. Hence, the arc OD (Fig. 8) including the origin O is part of the boundary of the footprint. But, if we restrict the footprint to the reachable domain, the locus of all terminal points where the speed reaches a prescribed value, say $u_f = w/\lambda_M$, then the boundary arc OD and its symmetric arc OF move away from the origin to the new boundary DEF. The lift program to reach this boundary always involves λ_M, but the bank angle computed from Eq. (8) alternatively changes its sign. It is simpler to see the improvement of the footprint with each switch by geometrical considerations. Let I be the switching point (Fig. 8), and assume that the trajectory is first flown with a left turn from O to I using the maximum permissible bank angle and then continues with a right turn with maximum bank. The trajectory terminates at the point F'. The two arcs ID and IF' are symmetric with respect to the velocity at the point I. Hence, the boundary connecting the limiting points D and F using one switch is obtained by following the locus of the

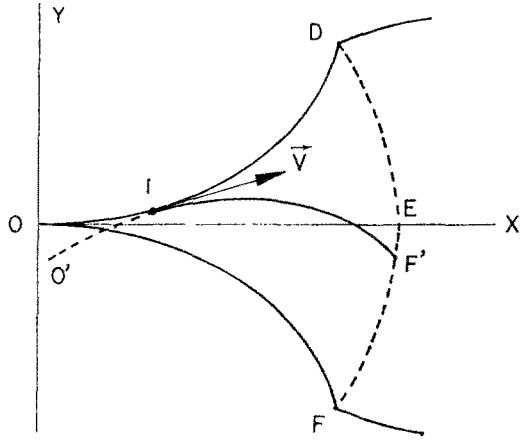

Fig. 8. Switching-in bank angle.

point F when we roll without slide the arc OF on the arc OD, and then use a symmetry with respect to the x-axis. Flight paths with two switches can be obtained by using the same geometric discussion; but, in this case of optimal coasting flight in a horizontal plane, a trajectory involving more than one switching has not been detected.

References

1. BUSEMANN, A., VINH, N. X., and CULP, R. D., *Optimum Altitude for Coasting Flight of a Hypervelocity Vehicle*, Journal of the Astronautical Sciences, Vol. 21, No. 1, 1973.
2. MIELE, A., *Flight Mechanics, Vol. 1: Theory of Flight Path*, Addison-Wesley Publishing Company, Reading, Massachusetts, 1962.
3. FAVE, J., *Approche Analytique du Problème du Domaine Accessible à un Planeur Orbital*, La Recherche Aérospatiale, No. 124, May-June, 1968.